であり，また，その持続時間はより長かった．UTPによるアロディニアは，P2受容体拮抗薬PPADSにより消失し，さらにPLC阻害剤U73122およびCaキレート剤BAPTA-AMによっても抑制される．これらの阻害様式は，DRG神経細胞でのUTPによる細胞内Ca^{2+}動員の阻害様式と一致しており，両者が同じP2Y受容体を介している可能性が示唆される．また，カプサイシン感受性神経破壊ラットでは，UTPによるアロディニアが抑制されることからも，カプサイシン感受性一次求心性神経（C線維）がUTPにより興奮し，アロディニアを惹起しているものと考えられる．この点も，*in vitro* の結果と一致している．候補として挙げられる責任受容体は，UTPに感受性の$P2Y_2$，$P2Y_4$，$P2Y_6$受容体である．しかし，$P2Y_6$受容体作用薬UDPはアロディニアを誘発しないことから，$P2Y_6$受容体の関与は考えにくい．さらに，$P2Y_2$受容体を減少させるためにラットの脊髄くも膜下腔内へ$P2Y_2$アンチセンスオリゴヌクレオチドを投与すると，UTPによるアロディニアはほぼ完全に抑制される．一方，$P2Y_4$アンチセンスオリゴヌクレオチドでは全く影響がない．したがって，UTPはC線維の$P2Y_2$受容体を介して，アロディニアを発現していることが示された．

3．痛み伝達のメカニズム

$P2Y_2$活性化が，いかにしてアロディニアを引き起こすかに関しては不明である．先行する報告で，Tominagaらは，P2Y受容体（$P2Y_1$あるいは$P2Y_2$）刺激によりTRPV1の応答の感受性が亢進すること[12]，また熱刺激に対する痛み行動が亢進すること[13]を報告している．つまり，P2Y受容体はTRPV1をエフェクターとして痛み情報を伝えているのである．P2Y受容体刺激によるTRPV1応答増強反応にはprotein kinase C（PKC）の活性化が必要だが，UTPによるアロディニアはPKC阻害薬に全く影響されず，さらにTRPV1阻害薬による影響も受けない．また，DRG神経細胞におけるカプサイシンによる$[Ca^{2+}]i$上昇もUTPで変化がないことから，UTPによるアロディニアには，TRPV1は関与していないと推察される（図4）．したがって，メカニカルアロディニア発現にはTRPV1感受性亢進とは別のメカニズムが関係している可能性が考えられる．またMolliverらは，$P2Y_2$受容体刺激により小型DRG神経細胞が脱分極し，活動電位を発生すること[14]，つまり$P2Y_2$受容体刺激が，痛み伝達に関わる小型DRG神経細胞を直接興奮させるというメカニズムを提唱している．交感神経節細胞の$P2Y_2$受容体でも同様のメカニズムが提唱されている．さらに，前述したように，大型DRG神経細胞には$P2Y_1$受容体が発現しており，この$P2Y_1$受容体が触刺激の応答亢進とリンクしている可能性が，アフリカツメガエル卵母細胞や，カエル下肢皮膚-感覚神経系で明らかにされている[7]．小型DRG神経細胞にも種々の機械応答センサーが存在していることから，同様のメカニズムが小型DRG神経細胞の$P2Y_2$受容体を介するシグナル経路に存在している可能性も考えられる．また，UTPは$P2Y_2$受容体を介して小型のDRG神経細胞で転写因子のCREB（cyclic AMP response element binding protein）を活性化する．これらの知見は，$P2Y_2$受容体が転写レベルでも痛みの伝達を制御している可能性を示唆するもので非常に興味深い．このように，小型のDRG神経細胞に存在しているP2Y受容体は，痛み伝達の調節に重要な役割を果たしているようであるが，その痛み伝達の調節メカニズムの詳細は，まだ不明な点も多く残されている．

一方，UTPおよびUDPは神経因性疼痛に対して抑制効果も有している．Okadaらは，UTPやUDPをラットの神経因性疼痛モデルで脊髄くも膜下腔内へ投与することで，神経損傷によるアロディニアが抑制されることを報告してい

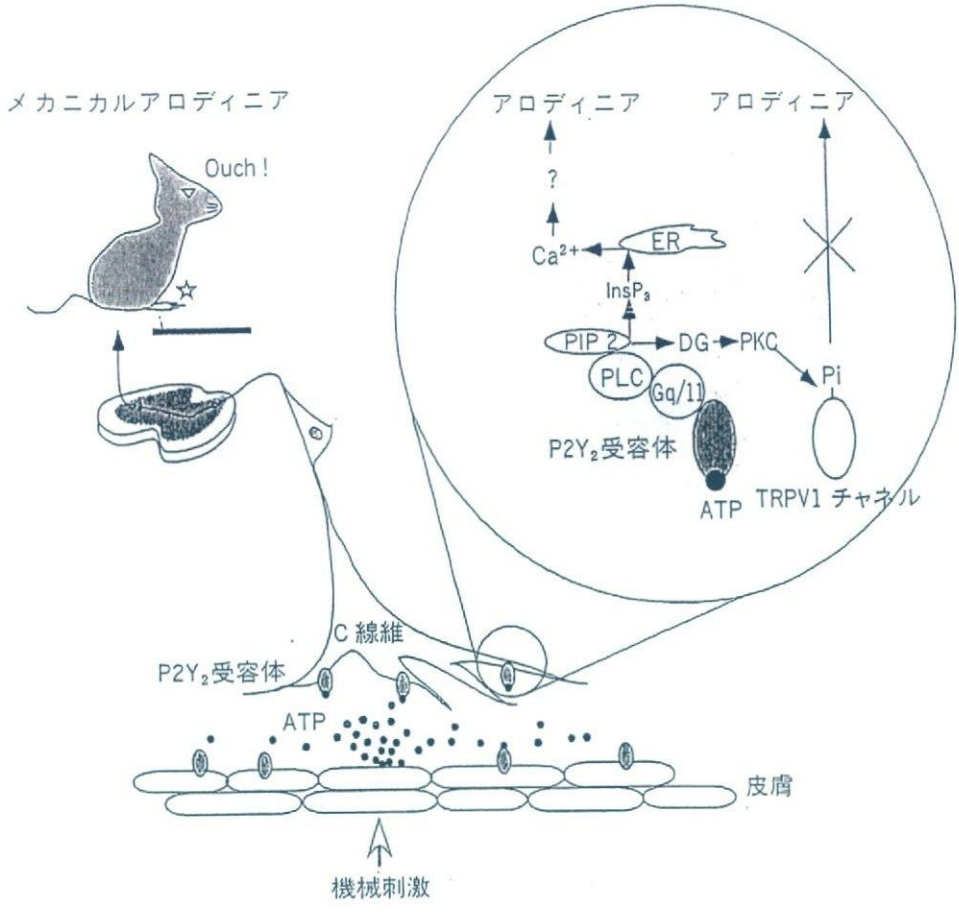

図4　まとめ（模式図）
皮膚は，機械刺激等の物理刺激および損傷等によりATPを放出する．一次求心性神経の末梢端はNHEKまで達していることから，知覚神経はしばしばATPに曝露される．一次求心性神経末梢端には，P2X受容体以外にP2Y受容体も存在し，特に無髄C線維には$P2Y_2$受容体が強く発現している．小型一次求心性神経$P2Y_2$受容体活性化によりメカニカルアロディニアが惹起される．この詳細な機序は不明であるが，PLCおよび細胞内Ca^{2+}が，その発現に重要な役割を果たす

る[15]．また，UTPおよびUDPは正常動物でも鎮痛効果を示す．このUTPとUDPの標的P2Y受容体が同一かどうかは不明だが，同じP2Y受容体系でも，脊髄$P2Y_6$受容体はむしろ鎮痛作用とリンクした分子である可能性が強い．

4．ATPのソースおよび周辺細胞とのコミュニケーション

一次求心性神経の末梢端は表皮ケラチノサイトにまで達している．また，先に述べたように，一次求心性神経はP2X受容体およびP2Y受容体を発現している．そこで，DRGとケラチノサイト（normal human epidermal keratinocytes：NHEKs）の共培養系を構築し，NHEKsとDRGのコミュニケーションの有無を検討した．Anti-peripherinおよびanti-cytokerain 14抗体を用いた二重染色法により，小型のC線維およびNHEKsが存在し，これらは互いに物理的に接触していることが明らかとなった（図

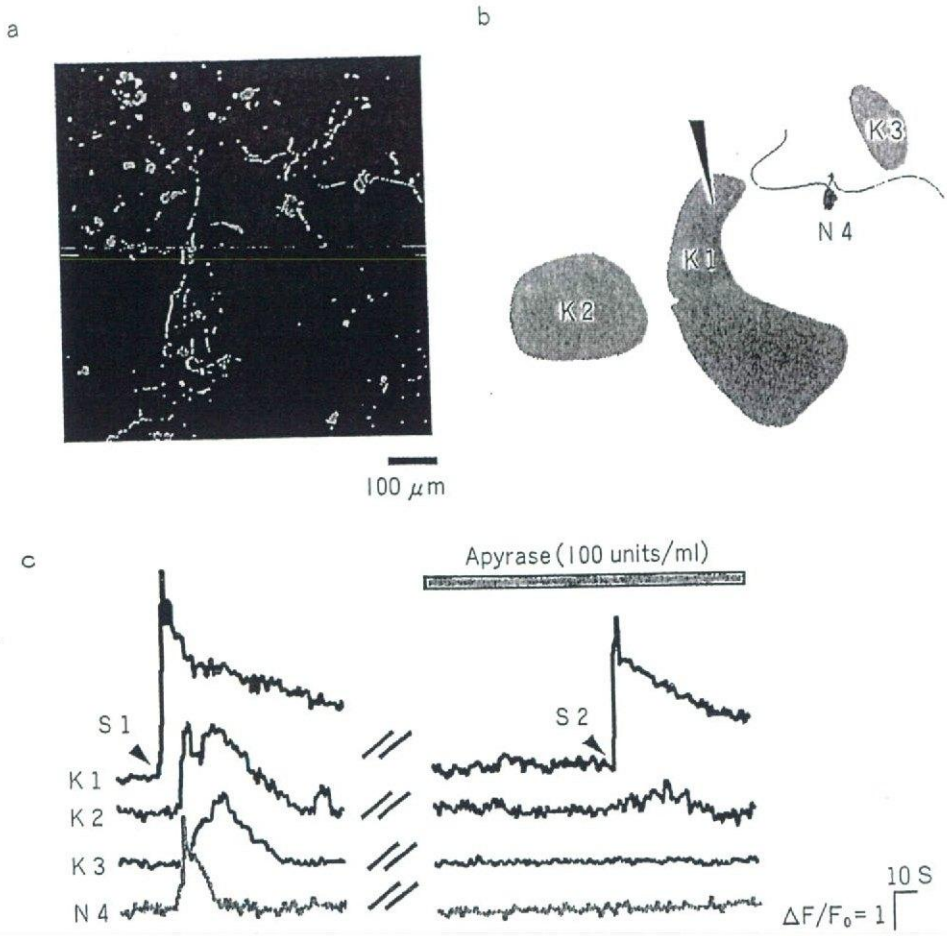

図5　ATPによるDRG神経ー表皮ケラチノサイト（NHEK）間コミュニケーション

a：DRG神経細胞およびNHEKの共培養系の免疫組織学像．小型DRG神経細胞はanti-peripherin抗体（緑），NHEKはanti-cytokeratin14抗体（赤）を用いて標識した．

b：NHEKの機械刺激（K1）により，その情報は離れたNHEKs（K2およびK3）へ，さらには近傍のDRG神経細胞（N4）にもCa^{2+}waveとして伝播した．

c：このCa^{2+}伝播は，ATP分解酵素apyraseによりほぼ消失した．$[Ca^{2+}]i$変動は共焦点レーザー顕微鏡によるfluo4法により測定し，値は⊿F/F0で表した

5 a)．この時，共培養細胞にKClで脱分極刺激を与えると，ほとんどのperipherin陽性DRG神経で$[Ca^{2+}]i$上昇が観察されたが，cytokeratin 14陽性NHEKsでは応答が観察されなかった．$P2Y_2$作用薬UTPで刺激を加えると，DRG神経でも，NHEKsでも$[Ca^{2+}]i$上昇が観察され，これはP2Y受容体の拮抗薬で抑制された．つまり小型DRG神経細胞およびNHEKs両者ともに機能的$P2Y_2$受容体を発現していることが明らかとなった．

ATPおよびそのアナログでNHEKsを刺激すると，ほとんどの細胞で$[Ca^{2+}]i$上昇が認め

られた．薬理学的な解析により，$P2Y_2$受容体がこの応答の主たる責任受容体であることが明らかとなった．ATPおよび$P2Y_2$受容体作用薬UTPによる$[Ca^{2+}]i$の上昇は，P2受容体拮抗薬により抑制された．次に内在性のATPにより同様の応答が観察されるか否かを検討した．あるNHEKに機械刺激を加えると，その細胞で$[Ca^{2+}]i$上昇が観察され，これはタイムラグを経て周囲のNHEKsへCa^{2+}waveとなって伝播した．このCa^{2+}wave伝播はP2受容体拮抗薬およびATP分解酵素apyrase存在下で，ほぼ消失する．したがって，機械刺激によるCa^{2+}waveの伝播には，ATPおよび$P2Y_2$受容体活性化が重要であること，つまり機械刺激に応答してATPが放出され，拡散し，周囲のNHEKsの$P2Y_2$受容体が活性化されることにより，Ca^{2+}waveが伝播されることが明らかとなった．また，ATPをルシフェリン・ルシフェラーゼ法とイメージング法の組み合わせにより画像化し[16]，実際に，NHEKsが機械刺激に応答してATPを放出していることも明らかとなった．

それでは機械刺激を受容したNHEKs細胞は，その刺激をATPの化学シグナルに変換して，DRG神経細胞にその情報を伝えることが可能なのであろうか？共焦点レーザー顕微鏡によるfluo4-Ca^{2+}イメージング法を用いた検討により，単一NHEKの機械刺激により，Ca^{2+}waveの伝播が近傍のDRG神経細胞に伝播すること，これがapyraseおよびsuraminにより抑制されたことから，NHEKsとDRG間のコミュニケーションがATP/$P2Y_2$受容体依存的に起きていることが明らかとなった（図5c）．Cookらは，DRG神経細胞と皮膚の共培養系を用い，皮膚を傷害すると，小型DRG神経細胞で，P2X受容体を介した内向き電流が観察されることを報告した[17]．これは，皮膚からのATPを介する情報が，P2X受容体を介した経路によってもDRG神経細胞に伝わることを示唆している．このように，皮膚は，一次求心性神経の自由終末にATPを供給する非常に大切なソースであると考えられる．また，皮膚は最も外側に位置する器官であり，身体を外界からの有害な刺激から守る役割を有しているが，それ以外に，外界からの物理刺激などの情報をATPの化学シグナルに変換して，知覚神経系に伝える重要な役割を有しているものと考えられる．また，DRG神経細胞の細胞体を取り巻くサテライトグリア細胞にも，$P2Y_1$および$P2Y_2$受容体が発現して，ATPを介してDRG神経細胞とコミュニケーションをとっている可能性があること[18]，中枢神経系ではアストロサイトがATPを放出して，周辺神経細胞およびグリア細胞の機能を調節していること[16]，などの報告から，部位によっては，グリア細胞がATPの供給源として，痛み伝達を制御する重要な細胞であると考えられる．

おわりに

ATPによる痛み情報の伝達について，特にP2Y受容体に関する最近の知見と，ATP/$P2Y_2$受容体を介した一次求心性神経-皮膚連関の重要性について述べた．表皮ケラチノサイトが，機械刺激に応答してATPを放出し，$P2Y_2$受容体を刺激することにより細胞間で情報を交換していること，さらに，このシグナルが皮膚に入力する小型一次求心性神経の$P2Y_2$受容体を活性化すること，DRG神経細胞$P2Y_2$受容体刺激がメカニカルアロディニアを引き起こす可能性を示した．皮膚は，通常の機械刺激だけでなく，傷害，紫外線照射などにより，容易にATPを放出する．ATPによるシグナルが，皮膚の機能だけでなく，皮膚-知覚神経細胞連関に強く影響すること，また，これまで痛覚伝達で注目されていたイオンチャネル型P2X受容体に加え，P2Y受容体も痛み情報の伝達と密接にリンクしている可能性が示唆された．ATPは，これら異なる

P2受容体群をどのように使い分けて痛み情報を伝達しているのか，また，異種P2受容体の相互作用によってどのように痛み情報が修飾されるのかなど，今後明らかにすべき課題は多く残されている．

文　献

1) Chen CC, Akopian AN, Sivilotti L, et al : A P 2X purinoceptor expressed by a subset of sensory neurons. Nature 377 : 428-431, 1995
2) Lewis C, Neidhart S, Holy C, et al : Coexpression of P2X2 and P2X3 receptor subunits can account for ATP-gated currents in sensory neurons. Nature 377 : 432-435, 1995
3) Tsuda M, Shigemoto-Mogami Y, Ueno S, et al : Downregulation of P2X3 receptor-dependent sensory functions in A/J inbred mouse strain. Eur J Neurosci 15 : 1444-1450, 2002
4) Tsuda M, Koizumi S, Kita A, et al : Mechanical allodynia caused by intraplantar injection of P2X receptor agonist in rats : involvement of heteromeric $P2X_{2/3}$ receptor signaling in capsaicin-insensitive primary afferent neurons. J Neurosci 20 : RC 90, 2000
5) Tsuda M, Shigemoto-Mogami Y, Koizumi S, et al : P2X4 receptors induced in spinal microglia gate tactile allodynia after nerve injury. Nature 424 : 778-783, 2003
6) Coull JA, Beggs S, Boudreau D, et al : BDNF from microglia causes the shift in neuronal anion gradient underlying neuropathic pain. Nature 438 : 1017-1021, 2005
7) Nakamura F, Strittmatter SM : P2Y1 purinergic receptors in sensory neurons : contribution to touch-induced impulse generation. Proc Natl Acad Sci USA 93 : 10465-10470, 1996
8) Sanada M, Yasuda H, Omatsu-Kanbe M, et al : Increase in intracellular Ca^{2+} and calcitonin gene-related peptide release through metabotropic P2Y receptors in rat dorsal root ganglion neurons. Neuroscience 111 : 413-422, 2002
9) Nakayama S, Yamashita T, Konishi M, et al : P2Y-mediated Ca^{2+} response is spatiotemporally graded and synchronized in sensory neurons : a two-photon photolysis study. Faseb J 18 : 1562-1564, 2004
10) Gerevich Z, Borvendeg SJ, Schroder W, et al : Inhibition of N-type voltage-activated calcium channels in rat dorsal root ganglion neurons by P2Y receptors is a possible mechanism of ADP-induced analgesia. J Neurosci 24 : 797-807, 2004
11) Gerevich Z, Muller C, Illes P : Metabotropic P2Y1 receptors inhibit P2X3 receptor-channels in rat dorsal root ganglion neurons. Eur J Pharmacol 521 : 34-38, 2005
12) Tominaga M, Wada M, Masu M : Potentiation of capsaicin receptor activity by metabotropic ATP receptors as a possible mechanism for ATP-evoked pain and hyperalgesia. Proc Natl Acad Sci USA 98 : 6951-6956, 2001
13) Moriyama T, Iida T, Kobayashi K, et al : Possible involvement of P2Y2 metabotropic receptors in ATP-induced transient receptor potential vanilloid receptor 1-mediated thermal hypersensitivity. J Neurosci 23 : 6058-6062, 2003
14) Molliver DC, Cook SP, Carlsten JA, et al : ATP and UTP excite sensory neurons and induce CREB phosphorylation through the metabotropic receptor, P2Y2. Eur J Neurosci 16 : 1850-1860, 2002
15) Okada M, Nakagawa T, Minami M, et al : Analgesic effects of intrathecal administration of P2Y nucleotide receptor agonists UTP and UDP in normal and neuropathic pain model rats. J Pharmacol Exp Ther 303 : 66-73, 2002
16) Koizumi S, Fujishita K, Tsuda M, et al : Dynamic inhibition of excitatory synaptic transmission by astrocyte-derived ATP in hippocampal cultures. Proc Natl Acad Sci USA 100 : 11023-11028, 2003
17) Cook SP, McCleskey EW : Cell damage excites nociceptors through release of cytosolic ATP. Pain 95 : 41-47, 2002
18) Weick M, Cherkas PS, Hartig W, et al : P2 receptors in satellite glial cells in trigeminal ganglia of mice. Neuroscience 120 : 969-977, 2003

※　　※　　※

Cellular and Molecular Neurobiology (© 2006)
DOI: 10.1007/s10571-006-9125-x

Inhibition of Transforming Growth Factor-β Production in Brain Pericytes Contributes to Cyclosporin A-Induced Dysfunction of the Blood-Brain Barrier

Fuyuko Takata,[1,2] Shinya Dohgu,[1] Atsushi Yamauchi,[1] Noriko Sumi,[1] Shinsuke Nakagawa,[2,3] Mikihiko Naito,[4] Takashi Tsuruo,[4] Hideki Shuto,[1] and Yasufumi Kataoka[1,2,5]

Received July 24, 2006; accepted October 5, 2006

SUMMARY

1. The present study was designed to clarify whether brain pericytes and pericyte-derived transforming growth factor-β1 (TGF-β1) participate in cyclosporin A (CsA)-induced dysfunction of the blood-brain barrier (BBB).

2. The presence of brain pericytes markedly aggravated CsA-increased permeability of MBEC4 cells to sodium fluorescein and accumulation of rhodamine 123 in MBEC4 cells.

3. Exposure to CsA significantly decreased the levels of TGF-β1 mRNA in brain pericytes in pericyte co-cultures. Treatment with TGF-β1 dose-dependently inhibited CsA-induced hyperpermeability and P-glycoprotein dysfunction of MBEC4 cells in pericyte co-cultures.

4. These findings suggest that an inhibition of brain pericyte-derived TGF-β1 contributes to the occurrence of CsA-induced dysfunction of the BBB.

KEY WORDS: Cyclosporin A; brain pericytes; transforming growth factor-β; blood-brain barrier; permeability; P-glycoprotein; mouse brain endothelial cells .

INTRODUCTION

Cyclosporin A (CsA), a cyclic 11-amino acid peptide, is widely used as a potent immunosuppressant to prevent allograft rejection in solid organ transplantation and in fatal graft-versus-host disease after bone marrow transplantation; it is also used to treat various autoimmune diseases including rheumatoid arthritis (Ka-

[1] Department of Pharmaceutical Care and Health Sciences, Faculty of Pharmaceutical Sciences, Fukuoka University, Jonan-ku, Fukuoka, 814-0180, Japan.
[2] PharmaCo-Cell Company Ltd., Nagayo-machi, Nagasaki, 851-2127, Japan.
[3] Department of Pharmacology 1, Nagasaki University School of Medicine, Sakamoto, Nagasaki, 852-8501, Japan.
[4] Institute of Molecular and Cellular Biosciences, University of Tokyo, Bunkyo-ku, Tokyo, 113-0032, Japan.
[5] To whom correspondence should be addressed; e-mail: ykataoka@fukuoka-u.ac.jp.

han, 1989). Despite its high efficacy, CsA has adverse effects including nephrotoxicity, cardiovascular disorders, gastrointestinal disorders and neurotoxicity. CsA-associated neurotoxicity occurs with a relatively high frequency (20–40%) in organ-transplanted patients with high blood drug levels or within the therapeutic range (The U.S. Multicenter FK506 Liver Study Group, 1994; Pirsch *et al.*, 1997; Gijtenbeek *et al.*, 1999). However, the mechanism of CsA-induced neurotoxicity remains obscure.

The entry of CsA into the brain is usually prevented by the tight junctions and P-glycoprotein (P-gp), a multi-drug efflux pump, of brain microvascular endothelial cells. But CsA-associated neurotoxicity, including tremors, seizures and encephalopathy, strongly suggests the possibility that CsA is transported across the blood-brain barrier (BBB). We previously reported that CsA produced convulsions by inhibiting γ-aminobutyric acid (GABA)ergic neural activity and the binding properties of the $GABA_A$ receptor (Shuto *et al.*, 1999). The inhibition of GABAergic neurotransmission by CsA may lead to an activation of serotonergic neural activity and, consequently, produce tremors (Shuto *et al.*, 1998). These *in vivo* findings are considered to be due to a direct action of CsA transported across the BBB rather than an indirect effect of CsA in the periphery. Indeed, we previously demonstrated that a high concentration of CsA decreased the function and expression of P-gp in brain capillary endothelial cells (Kochi *et al.*, 1999, 2000). The BBB is primarily formed from these cells, which are closely sealed by tight junctions (Pardridge, 1999). P-gp is abundantly expressed in brain endothelial cells and limits the accumulation of many hydrophobic molecules and toxic substances in the brain (Schinkel, 1999). Brain capillary endothelial cells are surrounded by two other cellular components of the BBB, astrocytes and brain pericytes. We also previously reported that the presence of astrocytes markedly aggravated CsA-induced hyperpermeability of, and P-gp dysfunction in, MBEC4 cells, through the acceleration of NO production (Dohgu *et al.*, 2004a). Brain pericytes are important for the growth and migration of endothelial cells and the integrity of microvascular capillaries (Thomas, 1999; Ramsauer *et al.*, 2002). Brain capillary endothelial cells communicate closely with brain pericytes to maintain the BBB (Hori *et al.*, 2004; Dohgu *et al.*, 2005). Transforming growth factor-β (TGF-β) is a cytokine produced by pericytes (Antonelli-Orlidge *et al.*, 1989). We previously reported that brain pericytes contribute to the up-regulation of barrier function and P-gp activity in brain endothelial cells through production of TGF-β1 (Dohgu *et al.*, 2005).

The present study was designed to clarify whether brain pericytes and pericyte-derived TGF-β participate in CsA-induced dysfunction of the BBB. We first evaluated the effect of CsA on the permeability of, and P-gp function in, mouse brain capillary endothelial (MBEC4) cells, either alone or co-cultured with human brain pericytes. Next, the effect of CsA on TGF-β1 mRNA expression in brain pericytes and the effect of TGF-β1 on CsA-decreased BBB function were examined in a co-culture system containing MBEC4 cells and brain pericytes.

MATERIALS AND METHODS

Materials

CsA was kindly supplied by Novartis Pharma (Basel, Switzerland). Sodium fluorescein (Na-F, MW 376), rhodamine 123 and human TGF-β1 were purchased from Sigma (St. Louis, MO). Culture medium and subculture reagents were obtained from Invitrogen (Carlsbad, CA). All remaining reagents of analytical grade were purchased from Wako (Osaka, Japan).

Cell Culture

MBEC4 cells, isolated from BALB/c mouse brain cortices and immortalized by SV40-transformation (Tatsuta *et al.*, 1992), were cultured in Dulbecco's modified Eagle's medium (DMEM) supplemented with 10% fetal bovine serum, 100 units/mL penicillin and 100 μg/mL streptomycin. Human brain pericytes (CS-ABI-499, Cell Systems Corporation, Kirkland, WA) were cultured in CS-C Complete Medium Kit (Cell Systems Corporation). They were grown in a humidified atmosphere of 5% CO_2/95% air at 37°C. To make an *in vitro* BBB model, brain pericytes (20,000 cells/cm^2) were first cultured in the wells of a 12-well culture plate. After 2 days, MBEC4 cells (42,000 cells/cm^2) were seeded on the inside of the collagen-coated polycarbonate membrane (1.0 cm^2, 3.0 μm pore size) of a Transwell®-Clear insert (12-well type, Costar, MA) placed in the plate containing layers of brain pericytes (pericyte co-culture). A monolayer system was also generated with MBEC4 cells alone (MBEC4 monolayer).

Cell viability was assessed using a WST-8 assay (Cell Counting Kit, DOJINDO, Kumamoto, Japan). The absorbance of a highly water-soluble formazan dye (WST-8), reduced by mitochondrial dehydrogenase, was measured in each sample at wavelengths of 450-nm (test wavelength) and 700-nm (reference wavelength).

Treatment with CsA and TGF-β1

TGF-β1 was dissolved in 4 mM HCl containing 1 mg/mL of bovine serum albumin; CsA was dissolved in ethanol. Each original solution was then diluted with serum-free medium. The final concentrations in the test media were 4 μM HCl/1 μg/mL bovine serum albumin or 0.1% ethanol. MBEC4 cells were cultured for 3 days, and the inserts were washed three times with serum-free medium. Cells were then exposed for 1–12 h to 5 μM of CsA injected into the inside of the insert (luminal side). Alternatively, TGF-β1 (0.01–1 ng/mL) was loaded on the luminal side. In parallel, cells were treated with serum-free medium containing the corresponding amount of ethanol and/or HCl and bovine serum albumin as the vehicle.

Transcellular Transport of Na-F

To initiate the transport experiments, the medium was removed and MBEC4 cells were washed three times with Krebs–Ringer buffer (118 mM NaCl, 4.7 mM KCl, 1.3 mM $CaCl_2$, 1.2 mM $MgCl_2$, 1.0 mM NaH_2PO_4, 25 mM $NaHCO_3$, and 11 mM D-glucose, pH 7.4). Krebs–Ringer buffer (1.5 mL) was added to the outside of the insert (abluminal side). Krebs–Ringer buffer (0.5 mL) containing 100 μg/mL of Na-F was loaded on the luminal side of the insert. Samples (0.5 mL) were removed from the abluminal chamber at 10, 20, 30 and 60 min and immediately replaced with fresh Krebs–Ringer buffer. Aliquots (5 μL) of the abluminal medium were mixed with 200 μL of Krebs–Ringer buffer and the concentration of Na-F was determined using a fluorescence multiwell plate reader (Ex(λ) 485 nm; Em(λ) 530 nm) (CytoFluor Series 4000, PerSeptive Biosystems, Framingham, MA). The permeability coefficient and clearance were calculated according to the method described by Dehouck *et al.* (1992). Clearance was expressed as microliters (μL) of tracer diffusing from the luminal to abluminal chamber and was calculated from the initial concentration of tracer in the luminal chamber and final concentration in the abluminal chamber: clearance (μL) = $[C]_A \times V_A/[C]_L$ where $[C]_L$ is the initial luminal tracer concentration, $[C]_A$ is the abluminal tracer concentration and V_A is the volume of the abluminal chamber. During the 60-min period of the experiment, the clearance volume increased linearly with time. The average volume cleared was plotted against time, and the slope was estimated by linear regression analysis. The slope of clearance curves for the MBEC4 monolayer or co-culture systems was denoted by PS_{app}, where PS is the permeability–surface area product (in μL/min). The slope of the clearance curve with a control membrane was denoted by $PS_{membrane}$. The real PS value for the MBEC4 monolayer and the co-culture system (PS_{trans}) was calculated as $1/PS_{app} = 1/PS_{membrane} + 1/PS_{trans}$. The PS_{trans} values were divided by the surface area of the Transwell inserts to generate the permeability coefficient (P_{trans}, in cm/min).

Functional Activity of P-gp

The functional activity of P-gp was determined by measuring the cellular accumulation of rhodamine 123 (Sigma) according to the method of Fontaine *et al.* (1996). MBEC4 cells were washed three times with assay buffer (143 mM NaCl, 4.7 mM KCl, 1.3 mM $CaCl_2$, 1.2 mM $MgCl_2$, 1.0 mM NaH_2PO_4, 10 mM HEPES, and 11 mM D-glucose, pH 7.4), and then incubated in 0.5 mL of assay buffer containing 5 μM rhodamine 123 for 60 min. The solution was then removed and the cells were washed three times with ice-cold phosphate-buffered saline and solubilized in 1 M NaOH (0.2 mL). The solution was neutralized with 1 M HCl (0.2 mL) and the rhodamine 123 content was determined using a fluorescence multiwell plate reader (Ex(λ) 485 nm; Em(λ) 530 nm, CytoFluor Series 4000). Protein concentration was measured by the method of Bradford (Bradford, 1976).

Expression of TGF-β1 Receptor mRNA in MBEC4 Cells and Human Brain Pericytes

Reverse-transcription polymerase chain reaction (RT-PCR) was employed to determine the level of mRNA expression for TGF-β1 receptor I and II in MBEC4 cells and brain pericytes. Total RNA was extracted from cultured cells using TRIzol™ reagent (Invitrogen, Carlsbad, CA) and 1 μg of RNA was reverse-transcribed and amplified by PCR using a SuperScript One-Step RT-PCR system (Invitrogen). Amplification was performed in a DNA thermal cycler (PC707; ASTEC, Fukuoka, Japan). The primers used and PCR conditions are summarized in Table I. Ten microliters of each PCR product was analyzed by electrophoresis on a 2% agarose (Sigma) gel with ethidium bromide staining. Gels were visualized on a UV light transilluminator and photographed using a DC290 Zoom digital camera (Kodak, Rochester, New York).

Relative Quantitation of TGF-β1 mRNA by Real-Time RT-PCR

Real-time RT-PCR was employed to determine the level of TGF-β1 gene expression in brain pericytes with CsA-treated pericyte co-culture. Total RNA was extracted from brain pericytes using TRIzol™ reagent (Invitrogen) and 2 μg RNA was reverse-transcribed using a SuperScript™ III First-Strand Synthesis System (Invitrogen) in a total volume of 20 μL, according to the manufacturer's protocol.

Real-time PCR was conducted on an Mx3000P™ Multiplex Quantitative PCR System (Stratagene, La Jolla, CA) with 2 μL of reverse-transcription product, Brilliant™ SYBR® Green QPCR Master Mix (Stratagene), primers at 150 nM and reference dye, in a total volume of 50 μL as per the manufacturer's protocol. The following PCR conditions were employed: 95°C for 10 min, followed by cycles of 95°C for 30 s, 54°C for 60 s and 72°C for 90 s. The sequences of primers were as follows: sense primer 5′-CCCTGGACACCAACTATTG-3′ and antisense primer 5′-CCGGGTTATGCTGGTTGTA-3′ for TGF-β1 (Untergasser *et al.*, 2005); sense primer 5′-GAGTCAACGGATTTGGTCGT-3′ and antisense primer 5′-TTGATTTTGGAGGGATCTCG-3′ for glyceraldehyde-3-phosphate dehydrogenase (GAPDH; GenBank Accession Number, M33197). After amplification, a melting curve was obtained by heating at 55°C and fluorescence data were collected at 0.2°C/s.

Relative quantitative analysis was performed employing Mx3000P™ Multiplex Quantitative PCR System software (Stratagene). We used the expression of GAPDH to normalize the expression data for the TGF-β1 gene. For a comparative analysis, values from vehicle treated brain pericytes were arbitrarily set as 1. Each sample was analyzed in triplicate.

Statistical Analysis

Values are expressed as means ± SEM. Statistical analysis was performed using Student's *t*-test. One-way and two-way analyses of variance (ANOVAs) followed by Tukey–Kramer's tests or Dunnett tests were applied to multiple com-

Table I Nucleotide Sequences of Probes Used in RT-PCR Assays and Amplification Conditions

Gene	Source (reference)	Sequence	Product (bp)	Amplification conditions
TGF-β R	Mouse (Machida *et al.*, 2000)	Sense 5′-ATCCATCACTAGATCGCCCT-3′ Antisense 5′-CGATGGATCAGAAGGTACAAGA-3′	824	94°C for 30 s, 57°C for 30 s, 72°C for 30 s
	Human (GenBank Accession Number, L11695)	Sense 5′-GATGGGCTCTGCTTTGTCTC-3′ Antisense 5′-CAAGGCCAGGTGATGACTTT-3′	214	94°C for 30 s, 54°C for 30 s, 72°C for 30 s
TGF-β R	Mouse (Machida *et al.*, 2000)	Sense 5′-CGTGTGGAGGAAGAACAACA-3′ Antisense 5′-TCTCAAACTGCTCTGAGGTG-3′	560	94°C for 30 s, 57°C for 30 s, 72°C for 30 s
	Human (GenBank Accession Number, E10743)	Sense 5′-TTTTCCACCTGTGACAACCA-3′ Antisense 5′-GGAGAAGCAGCATCTTCCAG-3′	185	94°C for 30 s, 54°C for 30 s, 72°C for 30 s

parisons. The differences between means were considered to be significant when P values were less than 0.05.

RESULTS

To obtain molecular evidence for the expression of TGF-β receptor I and II in MBEC4 cells and human brain pericytes, RT-PCR was carried out with a primer pair specific to each type of TGF-β receptor, from either mouse (for use on MBEC4 cells) or human (for use on human brain pericytes). As shown in Fig. 1A, RT-PCR with mRNA obtained from either MBEC4 cells or brain pericytes yielded a single product. The size of these products was as expected from the primer positions.

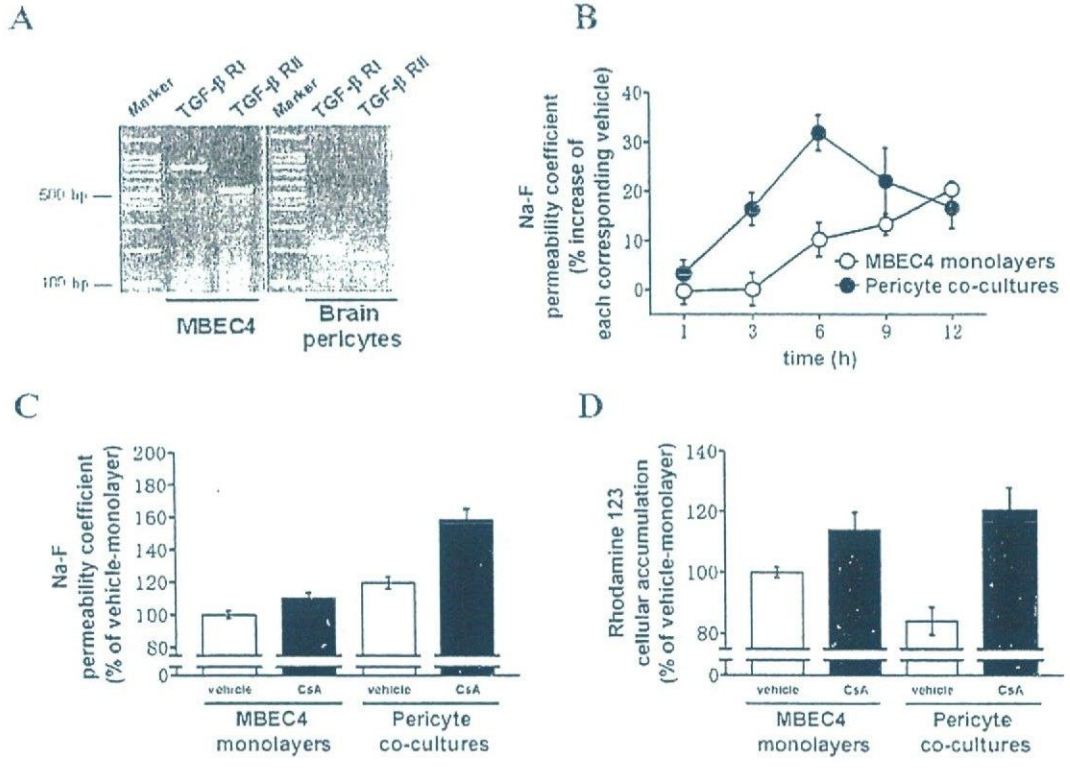

Fig. 1 (A) Expression of TGF-β receptor I and II mRNA in MBEC4 cells and human brain pericytes by RT-PCR analysis. (B) Time-course of the effect of CsA (5 μM) on the Na-F permeability of MBEC4 cells in MBEC4 monolayers and pericyte co-cultures. Transport experiments were performed after 1, 3, 6, 9 and 12 h of exposure to CsA. Results are expressed as % increase of each corresponding vehicle treatment (MBEC4 monolayers; $2.78 \pm 0.10 \times 10^{-4}$ to $3.47 \pm 0.14 \times 10^{-4}$ cm/min, pericyte co-cultures; $3.24 \pm 0.10 \times 10^{-4}$ to $4.47 \pm 0.20 \times 10^{-4}$ cm/min). Values are the means $\pm$ SEM (n = 7–16). (C) Effect of treatment with CsA (5 μM) for 6 h on the Na-F permeability of MBEC4 cells in MBEC4 monolayers and pericyte co-cultures. Results are expressed as % of vehicle-treated MBEC4 monolayers (% of vehicle-monolayer ($3.26 \pm 0.13 \times 10^{-4}$ cm/min)). Values are the means $\pm$ SEM (n = 7). (D) Effect of treatment with CsA (5 μM) for 6 h on the rhodamine 123 accumulation of MBEC4 cells in MBEC4 monolayers and pericyte co-cultures. Results are expressed as % of vehicle-treated MBEC4 monolayers (% of vehicle-monolayer (0.51 $\pm$ 0.12 nmol/mg protein)). Values are the means $\pm$ SEM (n = 8).

When MBEC4 cells were co-cultured with pericytes, the Na-F permeability of MBEC4 cells was increased from 3.26 ± 0.13 × 10^{-4} cm/min in monolayers to 3.86 ± 0.23 × 10^{-4} cm/min (Fig. 1C). The presence of pericytes decreased rhodamine 123 accumulation in MBEC4 cells from 0.51 ± 0.12 nmol/mg protein in monolayers to 0.43 ± 0.10 nmol/mg protein (Fig. 1D). A 12 h-exposure to CsA at 5 or 10 μM showed no effect on cell viability as determined by mitochondrial dehydrogenase activities (WST-8 assay) of MBEC4 cells in MBEC4 monolayers (100.0 ± 1.8 and 103.1 ± 7.8% of vehicle, respectively, $n = 4$ inserts) and pericyte co-cultures (99.2 ± 2.5 and 106.8 ± 2.3% of vehicle, respectively, $n = 4$ inserts). Figure 1C and D shows the effect of CsA (5 μM) on the permeability of MBEC4 cells to Na-F and the accumulation of rhodamine 123 in MBEC4 cells, respectively, in both MBEC4 monolayers and pericyte co-cultures. The Na-F permeability of MBEC4 cells was time-dependently increased during a period of 1–6 h after the addition of CsA (5 μM), reaching a peak at 6 h (Fig. 1B). A significant difference in CsA-induced hyperpermeability was observed between MBEC4 monolayers and pericyte co-cultures, with the effect being most apparent after a 6 h-exposure [$F(1, 24) = 10.51$, $P < 0.01$] (Fig. 1C). At the peak time, CsA increased the Na-F pearmeability of MBEC4 cells by 10.3 ± 3.4 and 31.9 ± 3.6% of each corresponding vehicle treatment in MBEC4 monolayers and pericyte co-cultures, respectively (Fig. 1C). Following exposure of cells to CsA for 9–12 h, permeability of the MBEC4 monolayers was gradually increased. However, the effect of CsA on pericyte co-cultures permeability became more moderate, reducing to the same level seen in MBEC4 monolayers (Fig. 1B). To clarify the role of brain pericytes in CsA-induced dysfunction of BBB, a 6 h-exposure of cells to CsA (5 μM) was employed in the following experiment. The accumulation of rhodamine 123 in MBEC4 cells was increased by 13.9 ± 5.9 and 43.4 ± 8.5% of each corresponding vehicle treatment in MBEC4 monolayers and pericyte co-cultures, respectively, after a 6 h-exposure to CsA (Fig. 1D). A significant difference in CsA-induced decrease in P-gp activity was observed between MBEC4 monolayers and pericyte co-cultures [$F(1, 28) = 4.65$, $P < 0.05$]. CsA-induced inhibition of P-gp function was more potent in pericyte co-cultures than in MBEC4 monolayers.

When pericyte co-cultures were treated with CsA (5 μM) for 6 h, the levels of TGF-β1 mRNA in brain pericytes were significantly decreased to 81.0 ± 7.3% of vehicle (Fig. 2A) [$F(2, 13) = 5.05$, $P < 0.05$]; however, a 12 h exposure to CsA failed to decrease levels of TGF-β1 mRNA in brain pericytes (103.8 ± 10.8% of vehicle). In pericyte co-cultures, TGF-β1 (0.01–1 ng/mL) dose-dependently inhibited the elevation of Na-F permeability (Fig. 2B), and rhodamine 123 accumulation (Fig. 2C), in MBEC4 cells, induced by CsA (132.9 ± 11.4 to 105.4 ± 2.5% and 140.3 ± 9.9 to 98.6 ± 6.4% of vehicle, respectively).

DISCUSSION

In the present study, CsA (5 μM) time-dependently increased the Na-F permeability of MBEC4 cells in pericyte co-cultures, this effect reaching a peak at 6 h

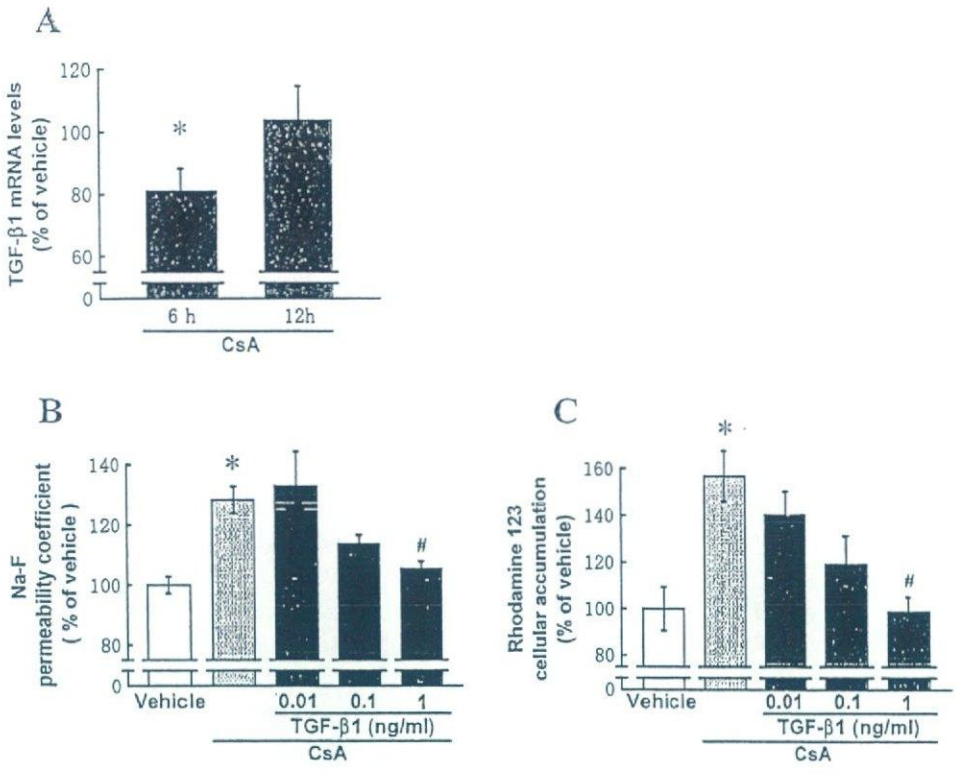

Fig. 2 (A) Effect of CsA (5 μM) on TGF-β1 mRNA expression in brain pericytes at 6 and 12 h after the addition of CsA in pericyte co-cultures. Total RNA of brain pericytes was extracted and subjected to real-time PCR analysis. Fold changes in TGF-β1 mRNA are normalized to GAPDH and compared with each corresponding vehicle treatment. Values are the means ± SEM (n = 3–5). $^{*}p < 0.05$, significant difference from vehicle. (B) Effect of TGF-β1 on CsA-increased Na-F permeability of MBEC4 cells in pericyte co-cultures. Results are expressed as % of vehicle (vehicle; 3.28 ± 0.22 × 10^{-4} cm/min). Values are the means ± SEM (n = 8–16). $^{*}p < 0.05$, significant differences from vehicle. $^{\#}p < 0.05$, significant difference from CsA treatment. (C) Effect of TGF-β1 on CsA-increased rhadamine 123 accumulation of MBEC4 cells in pericyte co-cultures. Results are expressed as % of each corresponding vehicle treatment (vehicle; 1.16 ± 0.24 nmol/mg protein). Values are the means ± SEM (n = 4–12). $^{*}p < 0.05$. significant differences from vehicle. $^{\#}p < 0.05$, significant difference from CsA treatment.

after the addition of CsA (Fig. 1B and C). A 6 h exposure to CsA also decreased P-gp function in MBEC4 cells in pericyte co-cultures, this effect being more apparent than that in MBEC4 monolayers (Fig. 1D). These findings suggest that CsA-induced hyperpermeability of, and P-gp dysfunction in, MBEC4 cells, was aggravated in pericyte co-cultures. We previously reported that treatment with CsA (0.5–10 μM) for 24 h dose-dependently decreased the viability of MBEC4 cells (Kochi *et al.*, 1999). The present study demonstrated that a 12 h-exposure to CsA at concentrations up to 10 μM had no effect on the viability of MBEC4 cells in MBEC4 monolayers and pericyte co-cultures. Thus, the exposure time (6 h) and the submaximum concentration (5 μM) of CsA without cytotoxicity were selected here.

The significance of brain pericytes in the regulation of the BBB was suggested by our previous study using a primary culture of rat brain pericytes. We reported

that brain pericyte-derived TGF-β1 contributed to the induction and up-regulation of BBB function (Dohgu *et al.*, 2004b, 2005). In the present study, the presence of human brain pericytes decreased the function of tight junctions and increased the function of P-gp, in MBEC4 cells, by about 20%. An interjunctional property of MBEC4 cells was lowered by co-culturing with human brain pericytes, this event being inconsistent with our previous report using a primary culture of rat brain pericytes. The different backgrounds of human brain pericytes commercially supplied and species-different cell type may be compounding factors in this discrepancy (Lai and Kuo, 2005); however, further studies are required to confirm this. Here, we employed a convenient *in vitro* model with MBEC4 cells and human brain pericytes.

To test whether TGF-β1 production of the brain pericytes participates in the mediation of CsA-induced dysfunction of the BBB, we examined the effect of CsA on the expression of TGF-β1 in brain pericytes. A 6 h exposure to CsA (5 μM) significantly decreased the levels of TGF-β1 mRNA in brain pericytes in pericyte co-cultures (Fig. 2A). Treatment with TGF-β1 dose-dependently inhibited CsA-induced hyperpermeability and P-gp dysfunction in MBEC4 cells in pericyte co-cultures (Fig. 2B and C). These findings suggest that CsA decreases BBB function by inhibiting TGF-β1 production in the brain pericytes. In pericyte co-cultures, an aggravation of CsA-induced hyperpermeability of MBEC4 cells occurred with a peak at 6 h after the addition of CsA, becoming more moderate at 9–12 h (Fig. 1B). In parallel with these events, TGF-β1 mRNA levels were significantly decreased by a 6 h exposure to CsA but not by a 12 h exposure (Fig. 2A), suggesting that CsA-induced hyperpermeability is ameliorated by the compensatory secretion of TGF-β1 from brain pericytes during the later period of CsA exposure. These data further support a critical role of pericyte-derived TGF-β1 in mediating CsA-induced BBB dysfunction.

RT-PCR analysis demonstrated the expression of TGF-β receptor I and II in MBEC4 cells and brain pericytes (Fig. 1A). TGF-β1 mRNA was also detected in brain pericytes (Fig. 2A) and MBEC4 cells (data not shown). Considering these observations, TGF-β is likely to participate in the up-regulation of BBB function through an autocrine and/or paracrine pathway in brain endothelial cells and pericytes. Autoinduction of TGF-β1 is mediated by binding of the transcription factor activator protein-1 (AP-1) complex to homologous elements in two regions of the TGF-β1 promoter (Kim *et al.*, 1990). In this positive autoregulation process, CsA is known to directly inhibit activation of the JunD isoforms in the AP-1 complex responsible for TGF-β signaling in lung fibroblasts (Eickelberg *et al.*, 2001). Calcineurin, a molecular target of CsA, has been shown to be involved in AP-1 activation in immune cells (Pfeuffer *et al.*, 1994; Tsuboi *et al.*, 1994). Based on this evidence, CsA may be interpreted as lowering TGF-β1 expression in brain pericytes due, at least in part, to an inhibition of the AP-1 activation step during TGF-β1 autoinduction. We previously reported that CsA increased NO production in MBEC4 cells (Dohgu *et al.*, 2004a) and elevated levels of NO have been known to reduce TGF-β1 production in the heart (Smith *et al.*, 2005). Therefore, CsA may also act on MBEC4 cells to lower TGF-β1 expression in brain pericytes.

In conclusion, CsA-induced hyperpermeability and P-gp dysfunction of MBEC4 cells were markedly aggravated in co-cultures with brain pericytes. This aggravation appears to occur due to CsA-induced inhibition of TGF-β1 expression in brain pericytes. These findings suggest that an inhibition of brain pericyte-derived TGF-β1 contributes to the occurrence of CsA-induced dysfunction of the BBB, thereby triggering neurotoxicity.

ACKNOWLEDGMENTS

This work was supported, in part, by Grants-in-Aid for Scientific Research ((B) 17390159) from JSPS, Japan and by a Grant-in-Aid for Exploratory Research (17659160) from MEXT, Japan. The authors thank Dr. Mária A. Deli (Institute of Biophysics, Biological Research Centre of the Hungarian Academy of Sciences) for pertinent comments on the manuscript.

REFERENCES

Antonelli-Orlidge, A., Saunders, K. B., Smith, S. R., and D'Amore, P. A. (1989). An activated form of transforming growth factor beta is produced by co-cultures of endothelial cells and pericytes. *Proc. Natl. Acad. Sci. U.S.A.* **86**:4544–4548.

Bradford, M. M. (1976). A rapid and sensitive method for the quantitation of microgram quantities of protein utilizing the principle of protein-dye binding. *Anal. Biochem.* **72**:248–254.

Dehouck, M.P., Jolliet-Riant, P., Bree, F., Fruchart, J. C., Cecchelli, R., and Tillement, J. P. (1992). Drug transfer across the blood-brain barrier: Correlation between *in vitro* and *in vivo* models. *J. Neurochem.* **58**:1790–1797.

Dohgu, S., Yamauchi, A., Nakagawa, S., Takata, F., Kai, M., Egawa, T., Naito, M., Tsuruo, T., Sawada, Y., Niwa, M., and Kataoka, Y. (2004a). Nitric oxide mediates cyclosporine-induced impairment of the blood-brain barrier in co-cultures of mouse brain endothelial cells and rat astrocytes. *Eur. J. Pharmacol.* **505**:51–59.

Dohgu, S., Yamauchi, A., Takata, F., Naito, M., Tsuruo, T., Higuchi, S., Sawada, Y., and Kataoka, Y. (2004b). Transforming growth factor-beta1 upregulates the tight junction and P-glycoprotein of brain microvascular endothelial cells. *Cell. Mol. Neurobiol.* **24**:491–497.

Dohgu, S., Takata, F., Yamauchi, A., Nakagawa, S., Egawa, T., Naito, M., Tsuruo, T., Sawada, Y., Niwa, M., and Kataoka, Y. (2005). Brain pericytes contribute to the induction and up-regulation of blood-brain barrier functions through transforming growth factor-beta production. *Brain Res.* **1038**:208–215.

Eickelberg, O., Pansky, A., Koehler, E., Bihl, M., Tamm, M., Hildebrand, P., Perruchoud, A. P., Kashgarian, M., and Roth, M. (2001). Molecular mechanisms of TGF-(beta) antagonism by interferon (gamma) and cyclosporine A in lung fibroblasts. *FASEB J.* **15**:797–806.

Fontaine, M., Elmquist, W. F., and Miller, D. W. (1996). Use of rhodamine 123 to examine the functional activity of P-glycoprotein in primary cultured brain microvessel endothelial cell monolayers. *Life Sci.* **59**:1521–1531.

Gijtenbeek, J. M., Van Den Bent, M. J., and Vecht, C. J. (1999). Cyclosporine neurotoxicity. *J. Neurol.* **246**:339–346.

Hori, S., Ohtsuki, S., Hosoya, K., Nakashima, E., and Terasaki, T. (2004). A pericyte-derived angiopoietin-1 multimeric complex induces occludin gene expression in brain capillary endothelial cells through Tie-2 activation *in vitro*. *J. Neurochem.* **89**:503–513.

Kahan, B. D. (1989). Cyclosporine. *N. Engl. J. Med.* **321**:1725–1738.

Kim, S. J., Angel, P., Lafyatis, R., Hattori, K., Kim, K. Y., Sporn, M. B., Karin, M., and Roberts, A. B. (1990). Autoinduction of transforming growth factor beta 1 is mediated by the AP-1 complex. *Mol. Cell. Biol.* **10**:1492–1497.

Kochi, S., Takanaga, H., Matsuo, H., Naito, M., Tsuruo, T., and Sawada, Y. (1999). Effect of cyclosporin A or tacrolimus on the function of blood-brain barrier cells. *Eur. J. Pharmacol.* **372**:287–295.

Kochi, S., Takanaga, H., Matsuo, H., Ohtani, H., Naito, M., Tsuruo, T., and Sawada, Y. (2000). Induction of apoptosis in mouse brain capillary endothelial cells by cyclosporin A and tacrolimus. *Life Sci.* **66**:2255–2260.

Lai, C. H., and Kuo, K. H. (2005). The critical component to establish *in vitro* BBB model: Pericyte. *Brain Res. Brain Res. Rev.* **50**:258–265.

Machida, H., Ogawa, K., Funaba, M., Mizutani, T., and Tsujimoto, M. (2000). mRNA expression of type I and type II receptors for activin, transforming growth factor-beta, and bone morphogenetic protein in the murine erythroleukemic cell line, F5–5.fl. *Eur. J. Endocrinol.* **143**:705–710.

Pardridge, W. M. (1999). Blood-brain barrier biology and methodology. *J Neurovirol.* **5**:556–569.

Pirsch, J. D., Miller, J., Deierhoi, M. H., Vincenti, F., and Filo, R. S. (1997). A comparison of tacrolimus (FK506) and cyclosporine for immunosuppression after cadaveric renal transplantation. FK506 Kidney Transplant Study Group. *Transplantation* **63**:977–983.

Pfeuffer, I., Klein-Hessling, S., Heinfling, A., Chuvpilo, S., Escher, C., Brabletz, T., Hentsch, B., Schwarzenbach, H., Matthias, P., and Serfling, E. (1994). Octamer factors exert a dual effect on the IL-2 and IL-4 promoters. *J. Immunol.* **153**:5572–5585.

Ramsauer, M., Krause, D., and Dermietzel, R. (2002). Angiogenesis of the blood-brain barrier *in vitro* and the function of cerebral pericytes. *FASEB J.* **16**:1274–1276.

Schinkel, A. H. (1999). P-Glycoprotein, a gatekeeper in the blood-brain barrier. *Adv. Drug Deliv. Rev.* **36**:179–194.

Shuto, H., Kataoka, Y., Kanaya, A., Matsunaga, K., Sueyasu, M., and Oishi, R. (1998). Enhancement of serotonergic neural activity contributes to cyclosporine-induced tremors in mice. *Eur. J. Pharmacol.* **341**:33–37.

Shuto, H., Kataoka, Y., Fujisaki, K., Nakao, T., Sueyasu, M., Miura, I., Watanabe, Y., Fujiwara, M., and Oishi, R. (1999). Inhibition of GABA system involved in cyclosporine-induced convulsions. *Life Sci.* **65**:879–887.

Smith, R. S., Jr., Agata, J., Xia, C. F., Chao, L., and Chao, J. (2005). Human endothelial nitric oxide synthase gene delivery protects against cardiac remodeling and reduces oxidative stress after myocardial infarction. *Life Sci.* **76**:2457–2471.

Tatsuta, T., Naito, M., Oh-hara, T., Sugawara, I., and Tsuruo, T. (1992). Functional involvement of P-glycoprotein in blood-brain barrier. *J. Biol. Chem.* **267**:20383–20391.

The U.S. Multicenter FK506 Liver Study Group. (1994). A comparison of tacrolimus (FK 506) and cyclosporine for immunosuppression in liver transplantation. *N. Engl. J. Med.* **331**:1110–1115.

Thomas, W. E. (1999). Brain macrophages: On the role of pericytes and perivascular cells. *Brain Res. Brain Res. Rev.* **31**:42–57.

Tsuboi, A., Muramatsu, M., Tsutsumi, A., Arai, K., and Arai, N. (1994). Calcineurin activates transcription from the GM-CSF promoter in synergy with either protein kinase C or NF-kappa B/AP-1 in T cells. *Biochem. Biophys. Res. Commun.* **199**:1064–1072.

Untergasser, G., Gander, R., Lilg, C., Lepperdinger, G., Plas, E., and Berger, P. (2005). Profiling molecular targets of TGF-b1 in prostate fibroblast-to-myofibroblast transdifferentiation. *Mech. Ageing Dev.* **126**:59–69.

Cellular and Molecular Neurobiology (© 2007)
DOI: 10.1007/s10571-007-9139-z

Rapid Communication

An Inhibitory Role of Nitric Oxide in the Dynamic Regulation of the Blood-Brain Barrier Function

Atsushi Yamauchi,[1] Shinya Dohgu,[1] Tsuyoshi Nishioku,[1] Hideki Shuto,[1] Mikihiko Naito,[2] Takashi Tsuruo,[2] Yasufumi Sawada,[3] and Yasufumi Kataoka[1,4]

Received June 2, 2006; accepted June 19, 2006

SUMMARY

1. The present study aimed at elucidating the effects of nitric oxide (NO) on blood-brain barrier (BBB) function with mouse brain capillary endothelial (MBEC4) cells.

2. Histamine (20–100 μM) evoked NO production (1.6–7 μM) in MBEC4 cells in a dose-dependent manner.

3. The permeability coefficient of sodium fluorescein for MBEC4 cells and the cellular accumulation of rhodamine 123 in MBEC4 cells were increased dose-dependently by addition of NO solutions (14 and 28 μM) every 10 min during a 30-min period.

4. The present study demonstrated that NO increased the permeability and inhibited the P-glycoprotein efflux pump of brain capillary endothelial cells, suggesting that NO plays an inhibitory role in the dynamic regulation of the BBB function.

KEY WORDS: nitric oxide; blood-brain barrier (BBB); permeability; P-glycoprotein; mouse brain endothelial cells.

INTRODUCTION

The blood-brain barrier (BBB) contributes to brain homeostasis and fulfills a protective function by regulating the access of solutes and toxic substances to the central nervous system. The BBB is formed by brain capillary endothelial cells, which are closely sealed by tight junctions (Pardridge, 1999). The tight junctions in the

[1] Department of Pharmaceutical Care and Health Sciences, Faculty of Pharmaceutical Sciences, Fukuoka University, 8-19-1 Nanakuma, Jonan-ku, Fukuoka 814-0180, Japan.
[2] Institute of Molecular and Cellular Biosciences, University of Tokyo, Bunkyo-ku, Tokyo 113-0032, Japan.
[3] Laboratory of Drug Informatics, Graduate School of Pharmaceutical Sciences, The University of Tokyo, 3-14-15 Hongo, Bunkyo-ku, Tokyo 113-0033, Japan.
[4] To whom correspondence should be addressed at Department of Pharmaceutical Care and Health Sciences, Faculty of Pharmaceutical Sciences, Fukuoka University, 8-19-1 Nanakuma, Jonan-ku, Fukuoka 814-0180, Japan; e-mail: ykataoka@fukuoka-u.ac.jp.

BBB prevent significant passive movement of small hydrophilic molecules from the blood to the brain, but specialized transport systems mediate the entry of essential substances such as glucose, amino acids, choline, monocarboxylic acids, amines, thyroid hormones, purine bases, and nucleosides (Tsuji and Tamai, 1999; Kusuhara and Sugiyama, 2001). The efflux transporter P-glycoprotein (P-gp) is a key element of the molecular machinery that confers special permeability properties on the BBB. P-gp, which was initially recognized for its ability to excrete anticancer drugs from multidrug-resistant cancer cells, is strongly expressed in brain capillaries. Its expression in the BBB limits the accumulation of many hydrophobic molecules and potentially toxic substances in the brain.

Nitric oxide (NO) is a transient product of inflammatory processes, generated from L-arginine by the enzyme NO synthase (NOS). NO appears to be involved in numerous vital cellular functions including neurotransmission, blood-pressure control, and the regulation of vascular tone. The basal production of NO appears to be required for biological regulation, and yet an excess of this same molecule can be cytotoxic to organism. But the molecular mechanisms mediating NO-induced tissue injury and breakdown of the BBB are not completely understood.

In the present study, to clarify the role of NO in the dynamic regulation of the BBB, we examined effects of NO on the function of tight junctions and P-gp in mouse brain capillary endothelial (MBEC4) cells. MBEC4 cells show the highly specialized characteristics of brain microvascular endothelial cells including P-gp expression (Tatsuta *et al.*, 1992, 1994).

MATERIALS AND METHODS

A saturated NO solution (typically containing approximately 1.4 mM NO) was prepared according to Ikesue *et al.* (2000). Deionized water (2 mL) was bubbled with argon for 20 min to remove oxygen. Then, the solution was bubbled with pure NO gas for 20 min and kept in a glass flask with a rubber septum under a NO atmosphere prior to use.

MBEC4 cells, which were isolated from BALB/c mouse brain cortices and immortalized by SV40-transformation (Tatsuta *et al.*, 1992), were cultured in Dulbecco's modified Eagle's medium (DMEM; GIBCO BRL, Life Technologies, Grand Island, NY) supplemented with 10% fetal bovine serum, 100 units/mL of penicillin, and 100 μg/mL of streptomycin. They were grown in 2.5-cm^2 dish, 12-well Transwells (Costar, MA) and 24-well plates in a humidified atmosphere of 5% CO_2/95% air at 37°C.

Direct and continuous electrochemical measurement of NO was performed with a three-electrode potentiostatic EMS-100 system (BIO-LOGIC, Grenoble, France), as previously described (Ikesue *et al.*, 2000; Trevin *et al.*, 1998). In brief, confluent MBEC4 cells in a 2.5-cm^2 dish were washed three times with Krebs–Ringer solution (143.0 mM NaCl, 4.7 mM KCl, 2.5 mM $CaCl_2$, 1.0 mM NaH_2PO_4, and 11.0 mM D-glucose, pH 7.4). The dish was placed on the stage of an inverted microscope (ECLIPSE TE300, Nikon, Tokyo, Japan) mounted with an NO monitoring

system. The NO-biosensor (ASTEC, Fukuoka, Japan) was positioned about 10 μm above the cell surface. Ten minutes after treatment with 1-mM L-arginine (Sigma, St. Louis, MO), histamine (Wako, Osaka, Japan) in a volume of 10 μL was added to the cells in 1 mL of Krebs–Ringer solution with a transient mixing step to give the final concentration indicated. The level of production of NO in MBEC4 cells was monitored for a 15-min period after the addition of histamine.

MBEC4 cells (42,000 cells/cm^2) were cultured on the collagen-coated polycarbonate membrane of the Transwell insert (3.0-μm pore size, 12-well type). After 3 days, they were washed three times with serum-free medium. Cells were exposed to 5 or 10 μL of NO solution (final concentration, 14 and 28 μM, respectively) injected into the inside of the insert (luminal side) every 10 min during a 30-min period. To initiate the transport experiments, the medium was removed, and cells were washed three times with Krebs–Ringer buffer (118 mM NaCl, 4.7 mM KCl, 1.3 mM $CaCl_2$, 1.2 mM $MgCl_2$, 1.0 mM NaH_2PO_4, 25 mM $NaHCO_3$, and 11 mM D-glucose, pH 7.4). Krebs–Ringer buffer (1.5 mL) was added to the outside of the insert (abluminal side). Krebs–Ringer buffer (0.5 mL) containing 100 μg/mL of sodium fluorescein (Na-F; Sigma) was loaded on the luminal side of the insert. Samples (0.5 mL) were removed from the abluminal chamber at 10, 20, 30, and 60 min and were immediately replaced with fresh Krebs–Ringer buffer. Aliquots (5 μL) from the abluminal chamber samples were mixed with 200 μL of Krebs–Ringer buffer, and then the concentration of Na-F was determined using a multiwell fluorometer ($E_x(\lambda)$ 485 nm; $E_m(\lambda)$ 530 nm; CytoFluor Series 4000, PerSeptive Biosystems, Framingham, MA). The permeability coefficient and clearance were calculated according to the method described by Dehouck *et al.* (1992). Clearance was expressed as microliters of tracer diffusing from the luminal to abluminal chamber and was calculated from the initial concentration of tracer in the luminal chamber and final concentration in the abluminal chamber: Clearance (μL) = $[C]_A \times V_A/[C]_L$ where $[C]_L$ is the initial luminal tracer concentration, $[C]_A$ is the abluminal tracer concentration, and V_A is the volume of the abluminal chamber. During a 60-min period of the experiment, the clearance volume increased linearly with time. The average volume cleared was plotted versus time, and the slope was estimated by linear regression analysis. The slope of clearance curves for the MBEC4 monolayer was denoted by PS_{app}, where PS is the permeability-surface area product (in microliters per minute). The slope of the clearance curve with a control membrane was denoted by $PS_{membrane}$. The real PS value for the MBEC4 monolayer (PS_{trans}) was calculated from $1/PS_{app} = 1/PS_{membrane} + 1/PS_{trans}$. The PS_{trans} values were divided by the surface area of the Transwell inserts to generate the permeability coefficient (P_{trans}, in centimeters per minute).

The functional activity of P-gp was determined by measuring the cellular accumulation of rhodamine 123 (Sigma) according to the method of Fontaine *et al.* (1996). MBEC4 cells (21,000 cells/cm^2) were cultured on collagen-coated 24-well plates. Three days after seeding, they were washed three times with serum-free medium and then exposed to 14–28 μM of NO solution every 10 min during a 30-min period. The medium was removed, and the cells were washed three times with assay buffer (143 mM NaCl, 4.7 mM KCl, 1.3 mM $CaCl_2$, 1.2 mM $MgCl_2$, 1.0 mM NaH_2PO_4, 10 mM HEPES, and 11 mM D-glucose, pH 7.4). The cells were incubated